UCRL-11424 Rev.

University of California

Ernest O. Lawrence Radiation Laboratory

PRODUCTION OF S = 0,-1 RESONANT STATES IN K^-p INTERACTIONS AT 2.45 GeV/c

Ronald R. Ross, Jerome H. Friedman, Daniel M. Siegel, Stanley Flatte, Luis W. Alvarez, Angela Barbaro-Galtieri, Janice Button-Shafer, Orin I. Dahl, Philippe Eberhard, William E. Humphrey, George R. Kalbfleisch, James S. Lindsey, Deane W. Merrill, Joseph J. Murray, Alan Rittenberg, Frank T. Shively, Gerald A. Smith, and Robert D. Tripp

July 7, 1964

Paper submitted to the 1964 International Conference on High Energy Physics, Dubna, U.S.S.R., August 5-15, 1964

UCRL-11424 Rev.

UNIVERSITY OF CALIFORNIA

Lawrence Radiation Laboratory
Berkeley, California

AEC Contract No. W-7405-eng-48

PRODUCTION OF $S = 0, -1$ RESONANT STATES IN $K^- p$ INTERACTIONS AT 2.45 GeV/c

Ronald R. Ross, Jerome H. Friedman, Daniel M. Siegel, Stanley Flatte, Luis W. Alvarez, Angela Barbaro-Galtieri, Janice Button-Shafer, Orin I. Dahl, Philippe Eberhard, William E. Humphrey, George R. Kalbfleisch, James S. Lindsey, Deane W. Merrill, Joseph J. Murray, Alan Rittenberg, Frank T. Shively, Gerald A. Smith, and Robert D. Tripp

July 7, 1964

PRODUCTION OF S = 0, -1 RESONANT STATES IN K^-p INTERACTIONS AT 2.45 GeV/c*

Ronald R. Ross, Jerome H. Friedman, Daniel M. Siegel, Stanley Flatte, Luis W. Alvarez, Angela Barbaro-Galtieri, Janice Button-Shafer, Orin I. Dahl, Philippe Eberhard, William E. Humphrey, George R. Kalbfleisch, James S. Lindsey, Deane W. Merrill, Joseph J. Murray, Alan Rittenberg, Frank T. Shively Gerald A. Smith, and Robert D. Tripp

(Presented by Ronald R. Ross)

Department of Physics and Lawrence Radiation Laboratory
University of California, Berkeley, California

July 7, 1964

I. INTRODUCTION

About 70 000 pictures of 2.45-GeV/c K^--p interactions have been obtained in the present 72-inch hydrogen bubble-chamber experiment.[1] Approximately 24 000 events of all topologies except 1-, 2-, and 3-prong events have been measured, and 50% have been remeasured. We report here on a study of the production of known resonances in the reactions:

$$K^- + p \rightarrow \Lambda + \pi^+ + \pi^- \qquad (1)$$

$$K^- + p \rightarrow \Lambda + \pi^+ + \pi^0 + \pi^- . \qquad (2)$$

The cross section for production and number of events in reactions (1) and (2) are given in Table I.

II. $Y_1^*(1385)$ AND ρ PRODUCTION IN THE REACTION $K^-p \rightarrow \Lambda\pi^+\pi^-$

To estimate the amount of resonance production, we have assumed no interference between production of Y_1^{*+}, Y_1^{*-}, ρ^0, or background. We constructed a likelihood function, assuming phase space for the nonresonant background and a matrix element proportional to $[(M - M_0)^2 + (\Gamma/2)^2]^{-1}$ for each resonant process, independent of any alignment. Masses and widths

---

*Work done under the auspices of the U. S. Atomic Energy Commission.

used in calculation of the likelihood function are given in Table II. The fit corresponding to the maximum likelihood is shown in Fig. 1 as a solid curve over histograms of the mass distribution of the events. In the $\Lambda\pi^-$ mass distribution the curve has been modified to take account of the nonisotropic decay of Y_1^{*+} with respect to its line of flight in the overall center of mass. We also show phase space, normalized to the total number of events, for comparison. The percentages of this final state contributed by each process are given in Table III. Even though interference may be important in further analysis of this final state, the mass distributions clearly do not give much information on this interference.

Figure 2 is a plot of the angular distribution in production of the three resonant states. We have defined a Y_1^* band as $\Lambda\pi$ invariant mass between 1.335 and 1.435 GeV/c^2 and a ρ band as $\pi^+\pi^-$ mass between 0.665 and 0.865 GeV/c^2 for selection of events to be included in angular distributions. For the Y_1^* production, Fig. 2a and b, the solid histogram corresponds to the angular distribution of those Y_1^* events that are not also in the ρ band. The dotted histogram is an estimate of the angular distribution for all Y_1^*; the contribution of events within the ρ band is estimated from Y_1^* events outside the ρ band that, upon a parity reversal of the Y_1^* in its center of mass, become events in the ρ band. This technique of treating the Y^*-ρ overlap region is described in reference 2.

In Fig. 2c, the solid histogram corresponds to all events in the ρ band. The dotted curve is an estimate of the angular distribution for ρ production arrived at by subtraction of background estimated by parity reversal of $\Lambda\pi$ events. This procedure is equivalent to assuming phase space for the non-Y_1^* events.

At this momentum the Y_1^{*+} and Y_1^{*-} angular distributions are markedly different from one another, and both distributions differ from previously reported angular distributions for the same states at lower momenta.[3] The ρ production angular distribution, after background subtraction is statistically very weak, and the forward peak is not statistically significant.

III. Y_1^*, ρ AND ω PRODUCTION IN THE REACTION $K^- p \to \Lambda \pi^+ \pi^0 \pi^-$

The effective-mass plots of this final state show significant evidence for the production of Y_1^*, ρ, and ω. Other resonant production occurs, but the rate of production is significantly lower than it is for these resonances. Again assuming (unjustifiably) noninterference of various resonant states and background, we have constructed a likelihood function similar to the one described in Section II for the eleven processes:

$$
\begin{aligned}
K^- p &\to \Lambda \omega \\
&\quad Y_1^{*+} \rho^- \\
&\quad Y_1^{*0} \rho^0 \\
&\quad Y_1^{*-} \rho^+ \\
&\quad Y^{*+} \pi^0 \pi^- \\
&\quad Y_1^{*0} \pi^+ \pi^- \\
&\quad Y_1^{*-} \pi^+ \pi^0 \\
&\quad \Lambda \pi^- \rho^+ \\
&\quad \Lambda \pi^0 \rho^0 \\
&\quad \Lambda \pi^+ \rho^- \\
&\quad \Lambda \pi^+ \pi^0 \pi^- .
\end{aligned}
$$

The masses and widths used in calculating the likelihood function are given in Table IV. The likelihood fits are not very sensitive to the widths used for the resonances; we find that 20% changes in the widths change the solutions by less than half a standard deviation. Table V gives the maximum likelihood

solution for percentages of the final state contributed by each process. Figure 3 contains mass plots for the two particle masses and the 3π system. Monte Carlo events were generated for each process. The solid curves of Fig. 3 are obtained from the Monte Carlo events by weighting each event in proportion to the appropriate percentage in Table III. Phase space normalized to the total number of events is shown as a dashed line in Fig. 3.

The π-π mass distributions at low π-π mass get a large contribution from the ω events ($\sim$300). For these events it was necessary to take account of the decay matrix element of the ω which sharpens the distribution of π-π masses.

The resonant production cross sections for Y_1^* and ω are about two times those reported by Bertanza et al. at this conference two years ago for K^- interactions at 2.24 GeV/c.[4] Their numbers were preliminary and based on 247 $\Lambda\pi^+\pi^0\pi^-$ events; so there is no real discrepancy.

Figure 4 gives the angular distribution in production of the $Y^*\rho$ and $\Lambda\omega$ events. If an event happened to fall in the overlap region of two $Y^*\rho$ charge combinations, it is not included in the angular distribution. There is no $Y^*\rho$ - $\Lambda\omega$ overlap. The $\Lambda\omega$ angular distribution is given with the Y_1^* events removed (solid curve) and with them included (dotted curve).

The $Y^*\rho$ and $\Lambda\omega$ angular distributions indicate that all kinematically allowed momentum transfers are involved in the production processes. The $Y^{*+}\rho^-$ events show a peaking at low momentum transfer, which may be due to the presence of an additional peripheral process. There is no significant change in the $\Lambda\omega$ angular distribution from that reported at 2.24 GeV/c by Bertanza et al.[4]

IV. CONCLUSION

We have determined the production cross section for the processes given in Tables III and V and angular distributions for the most copiously produced pseudo-two-body final states. It will be interesting to continue this procedure throughout the 2.0- to 2.8-GeV/c K^- momentum range for many final states

and try to relate the production cross sections by means of SU3 for different processes. For instance, the $Y_1^* \rho$ production should be related to the $\Xi^*(1530) K^*(888)$ production, since in each case we have a member of the well-known baryon decuplet and a member of the well-known vector-meson octet. At 2.45 GeV/c, the beam is below threshold for $\Xi^* K^*$ production; however, at 2.6 and 2.7 GeV/c $\Xi^* K^*$ production occurs.[5]

Table I. Cross sections and numbers of events for $K^- p \to \Lambda \pi^+ \pi^-$ and $K^- p \to \Lambda \pi^+ \pi^0 \pi^-$.

Reaction	Number of events	Cross section[a] (mb)
$K^- p \to \Lambda \pi^+ \pi^-$	576	0.68 ± 0.04
$K^- p \to \Lambda \pi^+ \pi^0 \pi^-$	1508	1.78 ± 0.07

a. Corrected for neutral Λ decay.

Table II. Masses and widths used in likelihood calculations for $K^- p \rightarrow \Lambda \pi^+ \pi^-$.

Resonance	Mass (GeV)	Width, Γ (GeV)
Y_1^{*+}	1.385	0.05
Y_1^{*-}	1.385	0.05
ρ^0	0.765	0.12

Table III. Maximum-likelihood solution for final-state contributions for each process for $K^- p \rightarrow \Lambda \pi^+ \pi^-$.

Reaction	Percent
$K^- p \rightarrow \Lambda \rho^0$	21.8 ± 3.7
$K^- p \rightarrow Y^{*+} \pi^-$	19.1 ± 2.3
$K^- p \rightarrow Y^{*-} \pi^+$	8.7 ± 1.9
"Phase space"	50.4 ± 4.1

Table IV. Masses and widths used in likelihood calculations for $K^- p \to \Lambda \pi^+ \pi^0 \pi^-$.

Resonance	Mass (GeV)	Width, Γ (GeV)
Y^{*+}	1.385	0.05
Y^{*-}	1.385	0.05
Y^{*0}	1.385	0.05
ρ^+	0.750	0.120
ρ^-	0.750	0.120
ρ^0	0.765	0.120
ω	0.782	0.035

Table V. Maximum-likelihood solution for final-state contributions for each process for $K^- p \to \Lambda \pi^+ \pi^0 \pi^-$.

Reaction	Percent
$K^- p \to \Lambda \omega$	21.5 ± 1.4
$K^- p \to Y^{*+} \rho^-$	12.0 ± 2.2
$K^- p \to Y^{*0} \rho^0$	5.0 ± 1.9
$K^- p \to Y^{*-} \rho^+$	10.7 ± 2.1
$K^- p \to Y^{*+} \pi^0 \pi^-$	6.4 ± 2.3
$K^- p \to Y^{*0} \pi^+ \pi^-$	8.5 ± 2.2
$K^- p \to Y^{*-} \pi^+ \pi^0$	4.7 ± 2.3
$K^- p \to \Lambda \pi^- \rho^+$	0(-1.9) ± 2.4
$K^- p \to \Lambda \pi^0 \rho^0$	3.8 ± 2.1
$K^- p \to \Lambda \pi^+ \rho^-$	3.4 ± 2.5
"Phase space"	25.8 ± 4.8

REFERENCES

1. J. J. Murray, J. Button-Shafer, F. T. Shively, G. H. Trilling, J. A. Kadyk, A. Rittenberg, D. M. Siegel, J. S. Lindsey, and D. W. Merrill. A Separated 2.5- to 2.8-GeV/c K^- Beam at the Bevatron, Lawrence Radiation Laboratory Report UCRL-11426, July 1964.
2. Philippe Eberhard and Morris Pripstein, Phys. Rev. Letters 10, 35 (1963).
3. Robert P. Ely, Sun-Yiu Fung, G. Gidal, Yu-Li Pan, W. M. Powell, and H. S. White, Phys. Rev. Letters 7, 461 (1961). J. Button-Shafer, D. Huwe, and J. J. Murray, "$\Lambda\pi^+\pi^-$ Final State in K^--p Interactions at K^- Momenta of 1.22 and 1.51 GeV/c," in Proceedings of the 1962 International Conference on High Energy Physics at CERN (CERN, Geneva, 1962), p. 303.
4. L. Bertanza, V. Brisson, P. L. Connally, E. L. Hart, I. S. Mittra, G. C. Moneti, R. R. Rau, N. P. Samios, I. O. Skillicorn, S. S. Yamamoto, M. Goldberg, L. Gray, J. Leitner, S. Lichtman and J. Westgard, "K^--p Interactions at 2.24 GeV/c II: Production Properties," in Proceedings of the 1962 International Conference on High Energy Physics at CERN (CERN, Geneva, 1962), p. 284.
5. G. A. Smith, J. S. Lindsey, and J. J. Murray, Production of $\Xi K(n)\pi$, $\Lambda K\bar{K}(n)\pi$, and $\Lambda K\bar{K}$ Final States in K^--p Interactions at 2.45 to 2.70 GeV/c, Lawrence Radiation Laboratory Report UCRL-11430, July 1964.

FIGURE LEGENDS

Fig. 1. Two-particle invariant-mass distributions for $\Lambda\pi^+\pi^-$ events. (Solid curve) likelihood fit; (dashed curve) phase space normalized to 576 events.

Fig. 2. Production angular distributions for

(a) $Y_1^{*+}(1385)$: (solid) no ρ; (dashed) adjusted total distribution (see text)

(b) $Y_1^{*-}(1385)$: (solid) no ρ; (dashed) adjusted total distribution (see text)

(c) ρ: (solid) all ρ; (dashed) adjusted total distribution (see text).

Fig. 3. Two-particle and $\pi^+\pi^0\pi^-$ invariant mass distributions for $\Lambda\pi^+\pi^0\pi^-$ events: (solid curve) Monte Carlo representation of the likelihood fit; (dashed curve) phase space normalized to 1508 events.

Fig. 4. Production angular distributions for pseudo-two-particle final states in the $\Lambda\pi^+\pi^0\pi^-$ final state. (See text for selection criteria.)

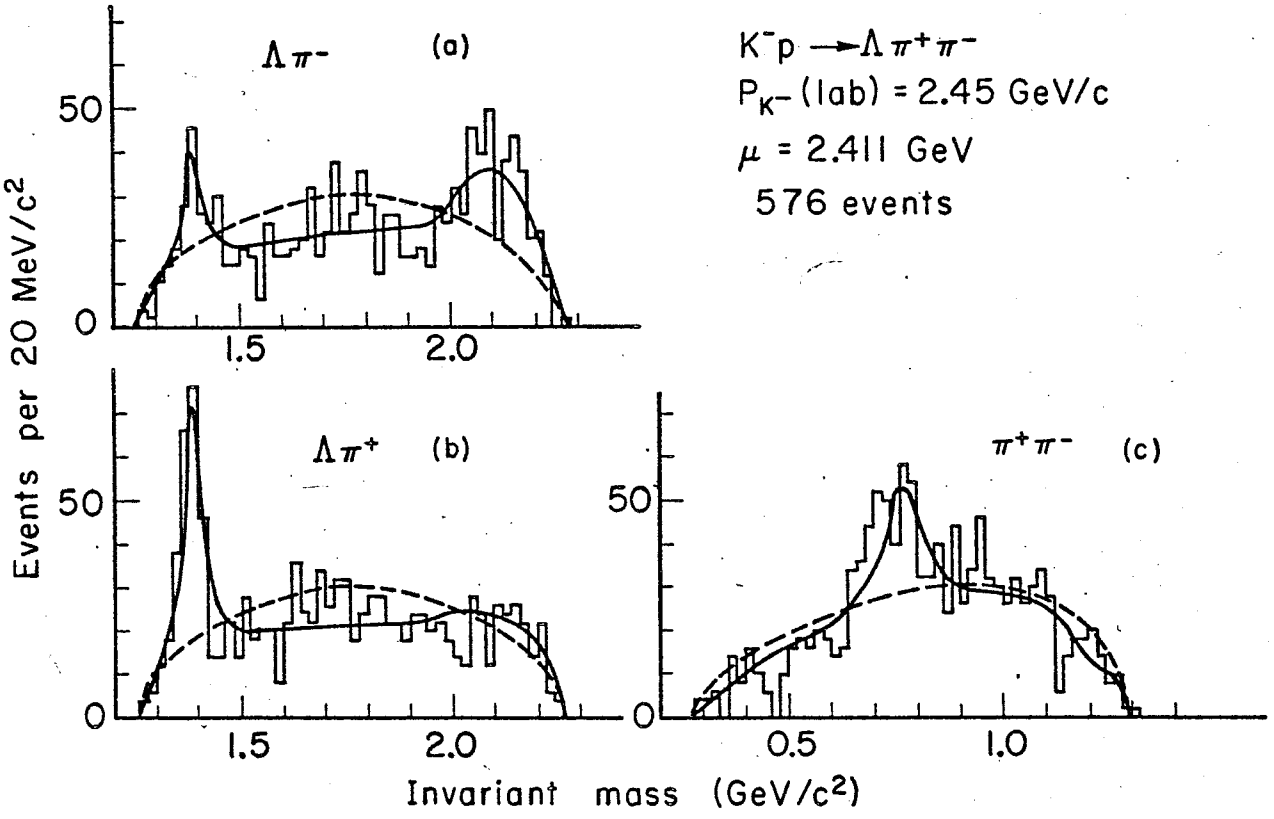

Fig. 1

MUB-3401

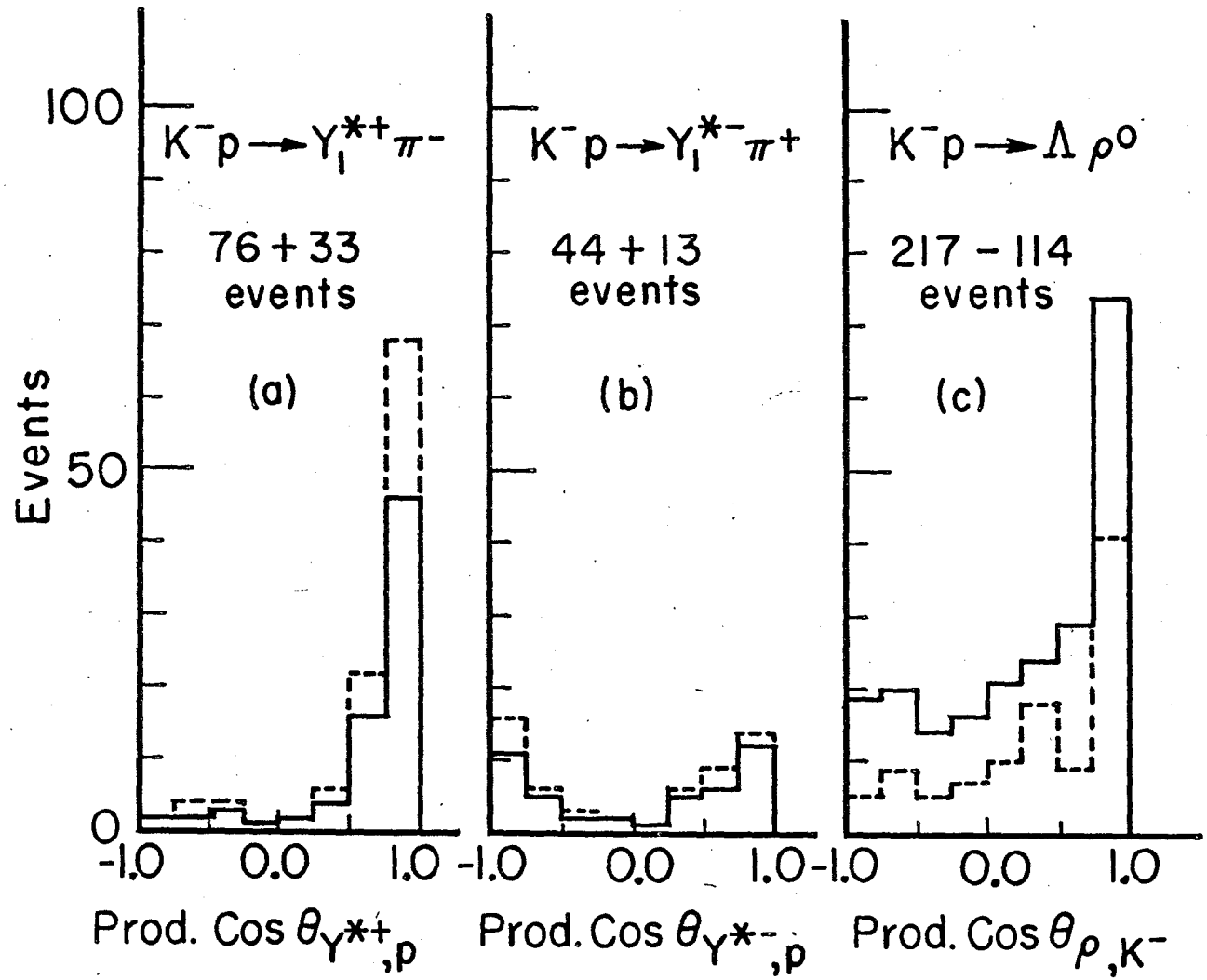

Fig. 2

MUB-3400

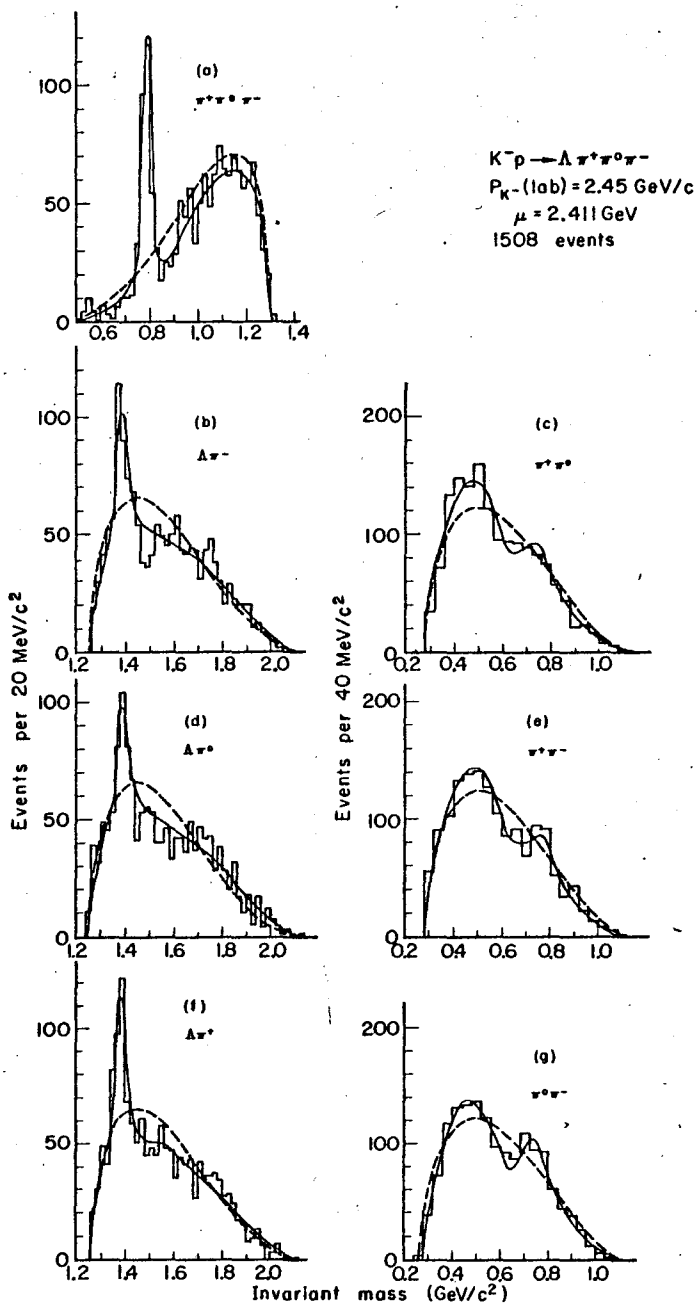
(a)
$\pi^+\pi^0\pi^-$
$K^-p \to \Lambda\pi^+\pi^0\pi^-$
P_{K^-}(lab) = 2.45 GeV/c
μ = 2.411 GeV
1508 events
(b)
$\Lambda\pi^-$
(c)
$\pi^+\pi^0$
(d)
$\Lambda\pi^0$
(e)
$\pi^+\pi^-$
(f)
$\Lambda\pi^+$
(g)
$\pi^0\pi^-$
Events per 20 MeV/c²
Events per 40 MeV/c²
Invariant mass (GeV/c²)
MUB-3402

Fig. 3

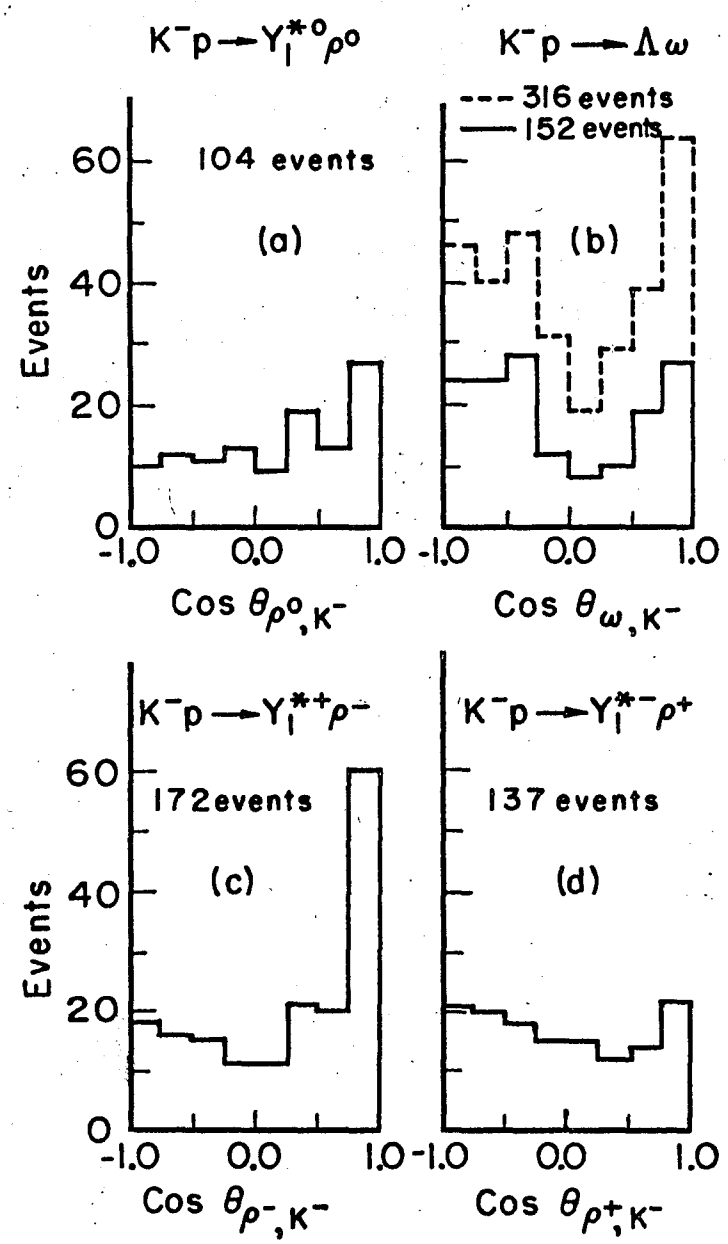

Fig. 4 MUB-3399